



Electrodeposited Bismuth Telluride Nanocomposite Thermoelectric Film with Improved Graphene Deposition

Muhammad Afiff Alias¹, Khairul Fadzli Samat^{1*}, Noraiham Mohamad¹, Mohd Warikh Abd Rashid¹, Mohd Asyadi Azam^{1,3}, Nguyen Van Toan², Takahito Ono², Alicja Klimkowicz³, Akito Takasaki³

¹ Fakulti Kejuruteraan Pembuatan, Universiti Teknikal Malaysia Melaka, 76100 Durian Tunggal, Melaka, Malaysia

² Department of Mechanical Systems Engineering, Tohoku University, Aoba-ku, Sendai 980-8579, Japan

³ Department of Engineering Science and Mechanics, Shibaura Institute of Technology, Toyosu Campus: 3-7-5, Toyosu, Koto-ku, Tokyo, 135-8548, Japan

ARTICLE INFO

Article history:

Received 27 July 2023

Received in revised form 29 September 2023

Accepted 15 October 2023

Available online 23 November 2023

Keywords:

Thermoelectric film; electrodeposition;
bismuth telluride; graphene;
nanocomposite

ABSTRACT

Thermoelectric (TE) films have become a prevalent research area due to their unique properties and potential applications in energy harvesting and waste heat recovery. Advancements in TE-materials development have been highlighted for the improved self-powered micro-device applications. (Advancements in TE materials have been developed for the improved self-powered micro-device applications.) In this paper, a detailed process of electrodeposition of Graphene/Bi₂Te₃ TE films by using a 3-electrode system potentiostat is presented. An improved suspension and dispersion of graphene in the 0.5-1.25 g/L graphene content electrolyte solution is prepared to attain better deposition of dispersed graphene in the nanocomposite film. The maximum deposition rate of the Graphene/Bi₂Te₃ films dropped more than half at 0.046 μm/min with 0.0185 A/cm² recorded current density as compared to the pristine Bi₂Te₃. Up to 3 wt.% of well dispersed and deposited graphene in the film have been successfully synthesized through -60mV pulsed deposition at room temperature. The average grain size of the Graphene/Bi₂Te₃ TE films decreased nearly 40% as compared to the pristine Bi₂Te₃ film. This work revealed that a smaller grain size and certain crystal defects formations for the synthesized nanocomposites. These could benefit TE properties of any TE materials by altering the electron mobility and phonons scattering.

1. Introduction

In recent decades, TE devices have gained considerable interest due to their unique properties, such as the capacity to directly convert heat into electricity. The increasing advancement of internet of things (IoT) technologies, energy harvesting and self-powered micro-macro devices could further drive the demand on the TE field. Nevertheless, the advancement of TE could be hindered due to limitations in fabrication methods and overall TE performance especially in TE film development. The evaluation of TE materials commonly employs the TE material figure of merit, ZT , which considers

* Corresponding author.

E-mail address: khairul.fadzli@utem.edu.my

<https://doi.org/10.37934/aram.111.1.161172>

the values of Seebeck coefficient (S), electrical conductivity (σ), and thermal conductivity (κ). However, TE films typically exhibit poor energy conversion efficiency, especially in applications near room temperature (300K). As a result, the overall TE material performance, as indicated by ZT , deteriorates even further in low-temperature applications [1].

Nanocomposites approach could increase TE performance by reducing thermal conductivity and boosting the material's electrical capabilities [2-4]. The use of nanostructured materials is required to increase the TE material performance such as promoting an electron properties configuration in reflect to Seebeck coefficient and electrical conductivity enhancements [2]. Nanocomposites are a type of nanostructured material system that contains nano-constituents in a matrix material or is a blend of various nanomaterials [3]. Nanocomposites provide interesting prospects to overcome certain limitations of existing TE materials. A unique optimization of the TE performance for every nanocomposite variation leads to the active development of high-performance TE films and devices.

The nanocomposites approach is a viable technique for increasing the TE performance through the point-plane defects and nano-structuring architecture of bismuth telluride (Bi_2Te_3)-based thin films [5]. Composites of Bi_2Te_3 nanoplates and carbon nanotubes produced a great TE performance with excellent flexibility [6]. The quality of the carbon nanotubes played an important role in increasing the TE performance of the nanocomposites [6]. The maximum Seebeck coefficient of the Bi_2Te_3 nanocomposite film with Pt nanoparticles inclusion can achieve 60% higher than the pure Bi_2Te_3 film in room application [7]. Although the observed electrical conductivity of the nanocomposite film decreased as the amount of deposited Pt nanoparticles grew, the expected power factor increased more than twice as much as the pristine film due to the high Seebeck coefficient and smaller grain size [7]. In 2022, Peigen Li *et al.*, presented an interfacial engineering technique for improving the TE performance of Bi_2Te_3 -based nanocomposites by incorporating graphene and a liquid-phase sintering procedure. The study found the nanocomposites had superior TE properties, including a greater Seebeck coefficient and decreased thermal conductivity [8].

The graphene inclusion in the Bi_2Te_3 -based TE films were proven capable in improving their TE performance [6,8-10]. However, there have been relatively few recent studies on graphene nanocomposites bismuth telluride TE film especially by using electrodeposition method. Moreover, the addition of graphene to Bi_2Te_3 can lead to a significant increase in electrical conductivity, thus increasing in conductivity can improve the overall TE performance of the material [11]. Furthermore, addition of graphene to Bi_2Te_3 can also lead to an increase in electron mobility which can improve the overall TE performance of the material [12].

In this study, an electrochemical deposition approach was used to synthesis Bi_2Te_3 nanocomposite TE films with several percentage of graphene inclusion. The main aim is to investigate the micro-structure and crystalline formation with respect to the benefit of TE performance. The electrodeposition process was controlled to produce a well dispersed graphene deposition. The inclusion of graphene into Bi_2Te_3 was proven to increase the electrical conductivity [12-13]. This is due to the fact that graphene can act as a conducting pathway for electrons, allowing them to move more freely through the material. Moreover, the addition of graphene nanocomposites in the Bi_2Te_3 could also improve electron mobility. The combination of reduced lattice thermal conductivity and increased electrical conductivity can lead to an overall improvement in the electron mobility of Bi_2Te_3 -based nanocomposites [13]. This improvement can be attributed to the decoupling of the electrical and thermal characteristics of the material, which allows for more efficient conversion of heat into electricity.

2. Methodology

2.1 Materials and Instruments

Bismuth oxide (Bi_2O_3) powders (99.999% trace metal base), tellurium dioxide (TeO_2) powders ($\geq 99\%$), nitric acid (65%), and graphene dispersion in N-methyl-2-pyrrolidinone (NMP) were acquired from Sigma-Aldrich. Meanwhile, a Potentiostat (Autolab PGSTAT 101) was used for the electrochemical deposition process. The surface morphology of the Graphene/ Bi_2Te_3 films was observed using field emission scanning electron microscopy (FESEM; JEOL JSM 7100F) and the elemental compositions were examined by using an energy-dispersive X-ray spectrometer (EDX) which was affiliated to the FESEM. The crystal orientation of Graphene/ Bi_2Te_3 and the size of its crystallites were studied using X-ray diffraction (XRD) patterns obtained from PANalytical X'PERT PRO with $\text{CuK}\alpha$ radiation ($\lambda = 1.54056 \text{ \AA}$). The nanostructured imaging of synthesized nanocomposite films was carried out by using transmission electron microscopy (TEM; JEOL JEM-2100) using 200kV voltage and were further analyzed using imageJ software.

2.2 Electrolyte Preparation

For the electrolyte solution, 1.0 M nitric acid (HNO_3) was used to dissolve the bismuth oxide (Bi_2O_3) and tellurium dioxide (TeO_2) powders. The mixing process was done in ultrasonic bath to enhance the dissolving of the powders. The electrolyte solution consisting of 3.2 mM Bi^{3+} and 7.2 mM HTeO_2^+ was mixed with desired concentration of graphene nanomaterials within 0.25 up to 01.25 g/L range (in the form of graphene-NMP solution). The mixing of the electrolyte with graphene-NMP was performed intermittently in ultrasonic bath and magnetic stirring for 2 hours. Figure 1 (a) shows the translucent electrolyte condition without the intermittent stirring-sonication procedure and the formation of agglomerated graphene in the solution can clearly be seen. In contrast, a stable and cloudy electrolyte can be observed when the graphene had successfully reached the dispersed and suspended conditions as shown in Figure 1 (b).

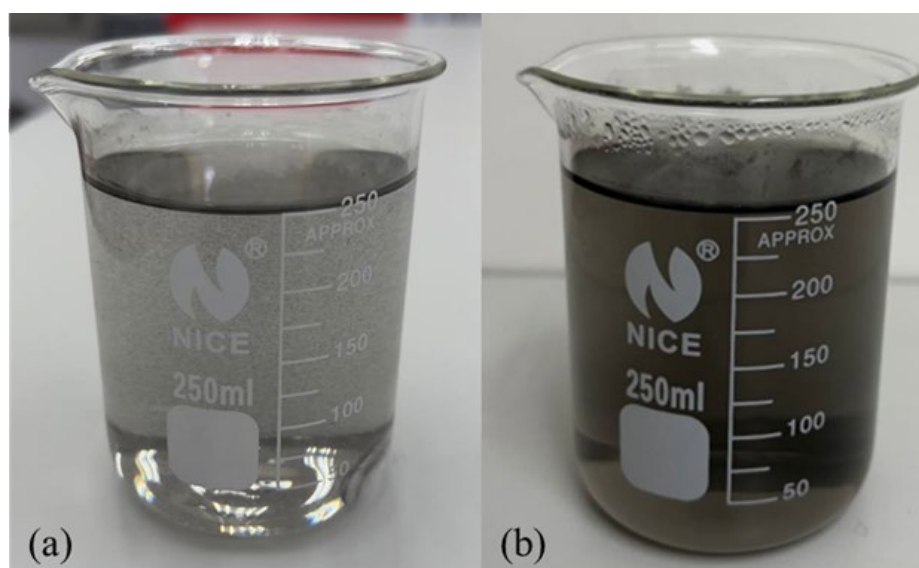


Fig. 1. (a) before and (b) after successful dispersion and suspension of graphene (1.25 g/L) in electrolyte solution

Using the intermittent method of mixing and sonication it was possible to avoid the aggregation of graphene and it led to a stable dispersion and suspension of graphene in the electrolyte solution.

The aggregated graphene dispersions can lead to non-uniform deposition of graphene on substrates [14]. The dispersion of the graphene was influenced by steric stabilization. It involves the introduction of steric repulsion between graphene sheets to prevent their restacking and aggregation, which is a common issue in graphene dispersions. Restacking can lead to reduced surface area and hinders the properties and performance of graphene-based materials [15].

2.3 Electrodeposition Parameter

Graphene/ Bi_2Te_3 nanocomposite films were synthesized by a three-electrode cell of electrochemical deposition system as illustrated in Figure 2. A computerized potentiostat instrument (PGSTAT101 Metrohm, AutoLab) linked to a computer equipped with software, NOVA 1.11 was employed for the deposition process. A Pt-strip electrode as (CE), an Ag/AgCl as reference electrode (RE) and a silicon substrate with a chromium-gold (Cr-Au) seed layer was used as a working electrode (WE). Electrodeposition process was potentiostatically carried out in a pulse deposition method at room temperature ($\sim 300\text{K}$). The thickness of the deposited films was maintained between $1\text{-}2\mu\text{m}$. The pulse cycle consisted of applying potential, E_{on} at a period, t_{on} and applying potential, E_{off} at a period, t_{off} . A rapid co-deposition occurred during 100 ms of t_{on} at applied potential -60 mV , E_{on} and no deposition happened during E_{off} period.

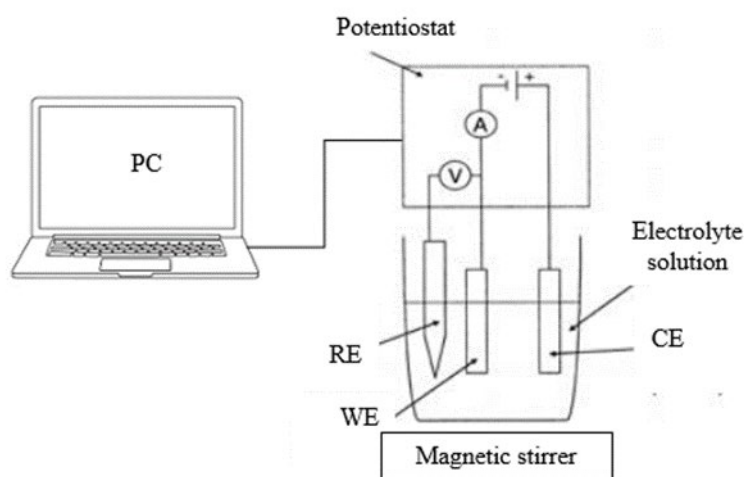


Fig. 2. Three-electrode system setup for electrodeposition

3. Results and Discussion

Figure 3 depicts the cyclic voltammograms (CVs) of the pristine Bi_2Te_3 (Solution I) and 1.25 g/L Graphene/ Bi_2Te_3 (solution IV). Cyclic voltammetry was performed on both Bi_2Te_3 and Graphene/ Bi_2Te_3 to investigate the oxidation-reduction (redox) reaction, particularly on the working electrode, and to establish the appropriate range of applied potential for electrodeposition. The values of reduction peak for the pristine Bi_2Te_3 and Graphene/ Bi_2Te_3 solutions were labeled as R1 and R2 respectively. There was a significant shift (negatively) for the reduction peak of the Graphene/ Bi_2Te_3 when compared to pristine Bi_2Te_3 . The shifting reduction should be due to the graphene co-deposition existence during the Bi_2Te_3 reduction. More electrons were transferred during the Bi_2Te_3 formation at the working electrode surface. The value of the reduction peak, R2 was recorded at -60mV and the R1 reached about -40mV .

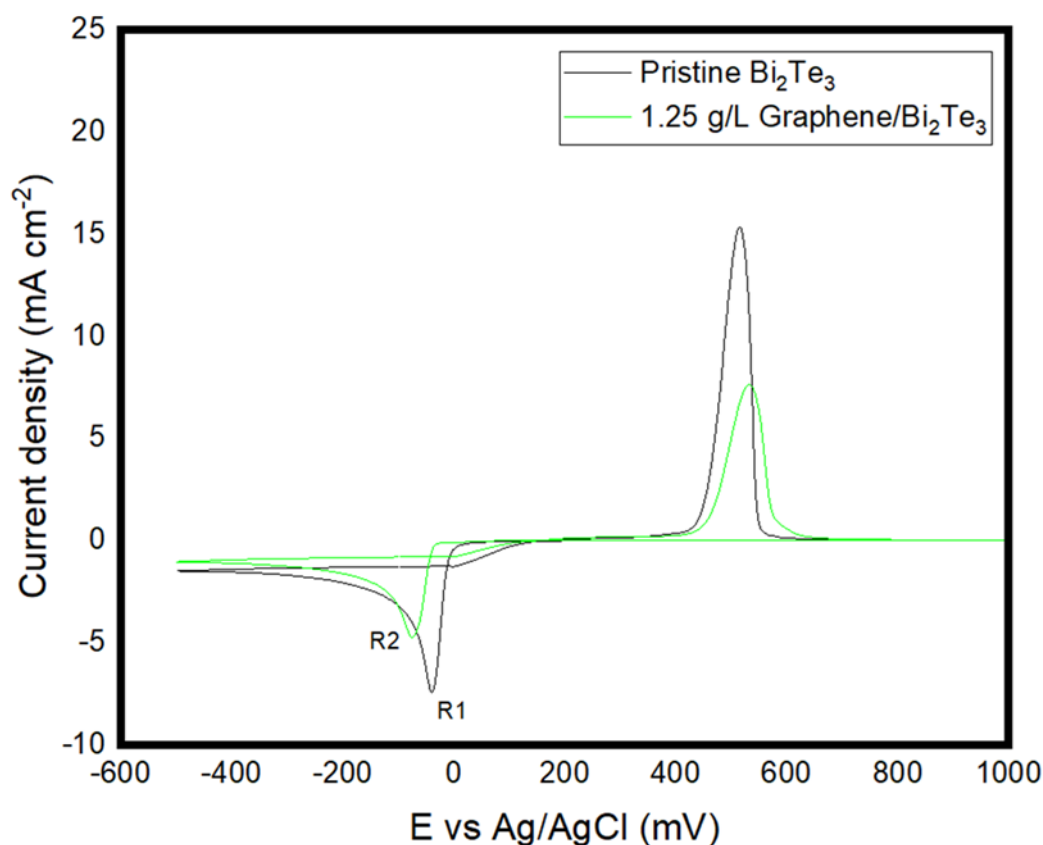


Fig. 3. Cyclic voltammograms of the pristine Bi_2Te_3 and 1.25 g/L Graphene/ Bi_2Te_3

The positively charged surface of NMP-coated graphene nanoparticles can promote stable electrolytic co-deposition by attracting negatively charged ions from the electrolyte solution. This results in the formation of a stable suspension of graphene nanoparticles in the solution, which can then be co-deposited with other materials such as Bi^{3+} and HTeO_2^+ during the electrodeposition process. The positively charged surface of the graphene nanoparticles is achieved by adsorption of metal ions on their surface, which leads to the formation of a positive charge on the surface of the nanoparticles [16]. This positive charge can attract negatively charged ions from the electrolyte solution, leading to the formation of a stable suspension of graphene nanoparticles in the solution. The stable suspension can then be co-deposited with other materials, leading to the formation of a composite material with enhanced properties. A fixed parameter of -60 mV (R2) was employed for all electrodepositions due to the improved morphological growth of the deposited films for both Graphene/ Bi_2Te_3 and Bi_2Te_3 .

Table 1 summarizes the compositions of elements in the Bi_2Te_3 and Graphene Bi_2Te_3 electrodeposited films. The composition was estimated using EDX. There were three electrolyte solutions with different graphene amounts (up to 1.25 g/L graphene content) and an electrolyte that did not contain any graphene at all. Using average values from an EDX measurement system, the amount of co-deposited graphene in the nanocomposite film was evaluated as C-wt.%. Up to 3.0 wt.% graphene has been successfully deposited in the nanocomposite film with reduced issues on the aggregated deposition.

Table 1

Element composition of electrodeposited films from EDX analysis

Electrolyte	Graphene content in electrolyte (g/L)	Electrodeposited film	Composition in the deposited film		
			Carbon (wt. %)	Bi:Te (at%)	Atomic percentage error due to Bi ₂ Te ₃ phase ratio (%)
I	0.00	Bi ₂ Te ₃	0.00	40:60	0
II	0.25	Graphene/ Bi ₂ Te ₃	1.20	42:58	± 2
III	0.75	Graphene/ Bi ₂ Te ₃	1.60	37:63	± 3
IV	1.25	Graphene/ Bi ₂ Te ₃	3.00	42:58	± 2

Steric repulsion between the graphene sheets creates an energy barrier that prevents their aggregation. This leads to improved dispersion stability, allowing the graphene sheets to remain dispersed and separated in the solvent [15]. Steric stabilization enables graphene dispersions development, allowing for uniform deposition and integration into different matrices [17]. It can enhance the compatibility of graphene with different solvents and matrices. This allows for the incorporation of graphene into various systems, including polymers, composites, and coatings, without compromising the stability and performance of the dispersion [18]. Low graphene dispersions in the electrolyte can lead to poor quality of graphene deposited with defects and impurities existences, which can affect the performance of graphene-based devices [19]. In addition the aggregated problems of graphene nanocomposites in the electrolyte solution could cause the deposited films with a low weight percentage of graphene nanocomposites [20]. As the graphene content increases in the electrolyte, the amount of deposited graphene in the film increases. The atomic percentage error for Bi-Te ratio was highly acceptable which is not more than 3% error based on the perfect ratio of Bi₂Te₃ (40:60). The ratio variation of Bi-Te should be no more than 5% of error from the pristine one to avoid any possible factor of ratio effect in the TE performance [21].

Typical growth of pristine Bi₂Te₃ surface-crystals structure known as plate-like structure or also called needle-like structure is shown in Figure 4 (a). The micro-structure of the nanocomposite film Figure 4 (b), (c) and (d) showed a typical needle-like shape but much smaller in size compared to the pristine Bi₂Te₃ [22-23]. The change of size was due to the inclusion of graphene in the Bi₂Te₃ matrix that affected the size of crystal structure. Smaller structural growth typically results in reduced pore size and a more compact surface structure and thus minimizing porosity could lead to an enhancement in electrical conductivity due to the [24]. The investigation of electrical characteristics in Bi₂Te₃ thin films indicates that as the charge carrier concentration rises, so does the electrical conductivity [24].

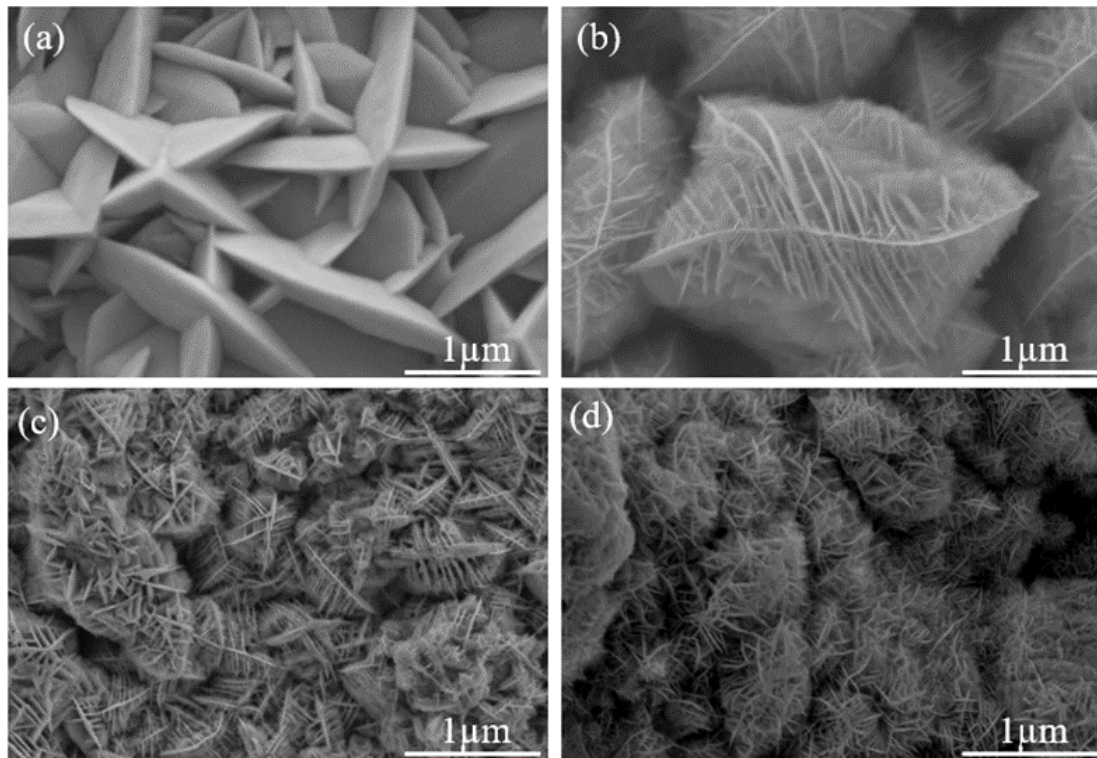


Fig. 4. FESEM micrograph image of deposited films (a) Bi_2Te_3 ; (b) 1.2 wt.% Graphene/ Bi_2Te_3 ; (c) 1.6 wt.% Graphene/ Bi_2Te_3 ; 3.0 wt.% Graphene/ Bi_2Te_3

Figure 5 depicts the X-Ray patterns of deposited film that contains graphene inclusion with Bi_2Te_3 up to 2.7 wt.%. The analysis of the diffraction data obtained from the XRD indicated that the deposited films showed rhombohedral crystal structure ($R\bar{3}m$). As observed in the patterns, the (015), (1010) and (110) peaks were observed and the results are in agreement with the ones reported by Hosokawa *et al.*, [25-27]. Through the incorporation of a higher weight percentage of graphene into the nanocomposite, a reduction in the grain size of Bi_2Te_3 was confirmed. The average grain size was determined by analyzing the Full Width at Half Maximum (FWHM) and the Integral Breadth, β values of the Bi_2Te_3 peaks, and then calculated using the Scherrer equation.

Crystallites grain size within a polycrystalline material are relatively uniform in size and distribution, then the crystallite size can indeed be comparable to the grain size. The grain size was reduced by adding more graphene to the nanocomposite as shown in Table 2. The smallest grain size was calculated to be approximately 20.56 nm, which was roughly 40% smaller than the pure Bi_2Te_3 film. The significant enhancement in ZT (figure of merit for TE materials) is achievable via grain size reduction [28]. Consistently, the electrical resistivity of bulk nanograined Bi_2Te_3 material increases as the grain size decreases, suggesting that smaller grain size can lead to the reduction of electrical conductivity [29], and increases the density of grain boundary formation which could simultaneously increase the scattering of heat carriers such as phonons and electrons [30]. It is conceivable that the increased scattering disrupts the coherent propagation of heat and reduces thermal conductivity. The phonons scattering was enhanced because smaller grain size yields a higher abundance of grain boundaries, which induces phonon scattering due to lattice misalignment at the grain boundaries [31].

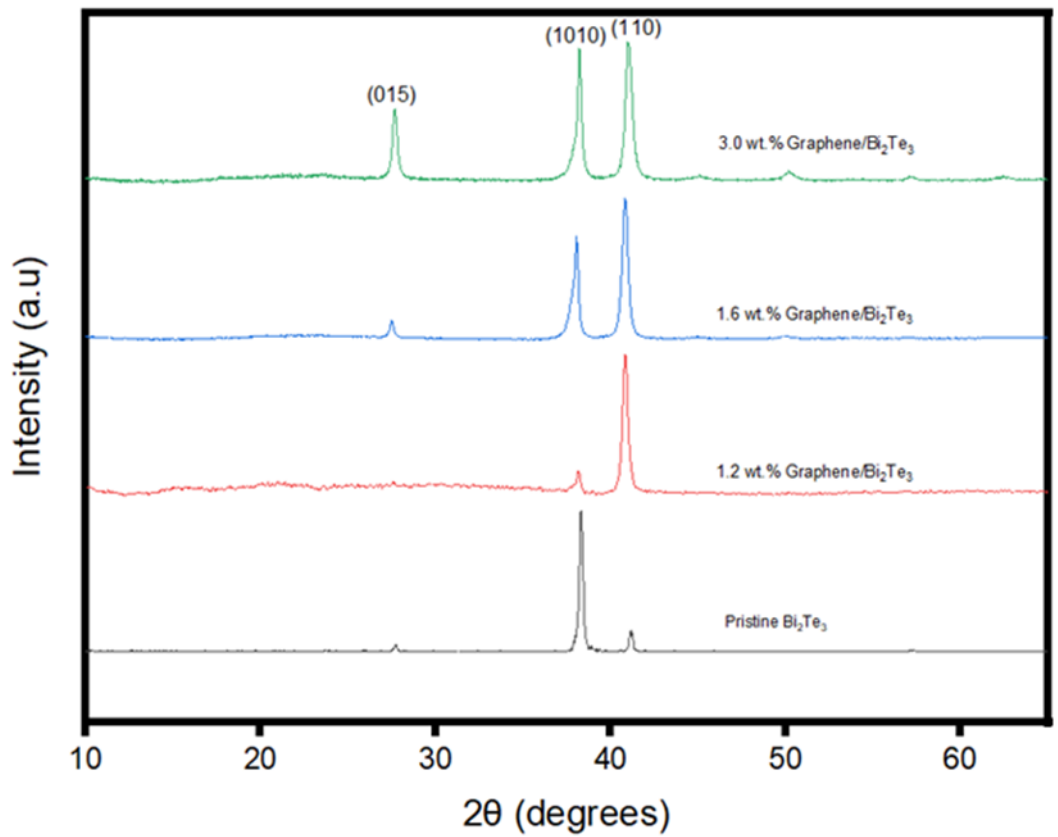


Fig. 5. XRD results for the electrodeposited film

Table 2

Summary of average crystallite grain size and of the deposited film

Film type	Integral Breadth, β at $2\theta = 41.2^\circ(\text{rad})$	Average crystallite grain size (nm)
Bi ₂ Te ₃	4.80×10^{-3}	34.7 ± 1.0
1.2 wt.% Graphene/Bi ₂ Te ₃	4.96×10^{-3}	25.8 ± 1.0
1.6 wt.% Graphene/Bi ₂ Te ₃	5.56×10^{-3}	24.8 ± 1.0
3.0 wt.% Graphene/Bi ₂ Te ₃	5.81×10^{-3}	20.6 ± 1.3

TEM image of imperfect crystalline lattice graphene nanomaterials in the Bi₂Te₃ matrix deposited with dispersed and suspend electrolyte solutions is shown in Figure 6 (a). The crystal structure rhombohedral from XRD data reconfirms the results from the TEM image as the crystal structure exhibits polycrystalline materials. Moreover, Figure 6 (b) depicts the spotty ring pattern in the selected area electron diffraction (SAED) with hkl (015), (1010) and (110) which was calculated by using ImageJ software. This spotty ring pattern is commonly observed in polycrystalline materials, where diffracting hkl planes are oriented randomly in all directions as shown in Figure 6 (a) [32]. The presence of crystal defects Figure 6 (a), such as stacking faults (D3) and vacancy defects (D1 and D2), can cause the spotty ring pattern to appear stretched or irregular [33]. TE properties especially in thermal conductivity can be further optimized by understanding the formation and behavior of defects [34].

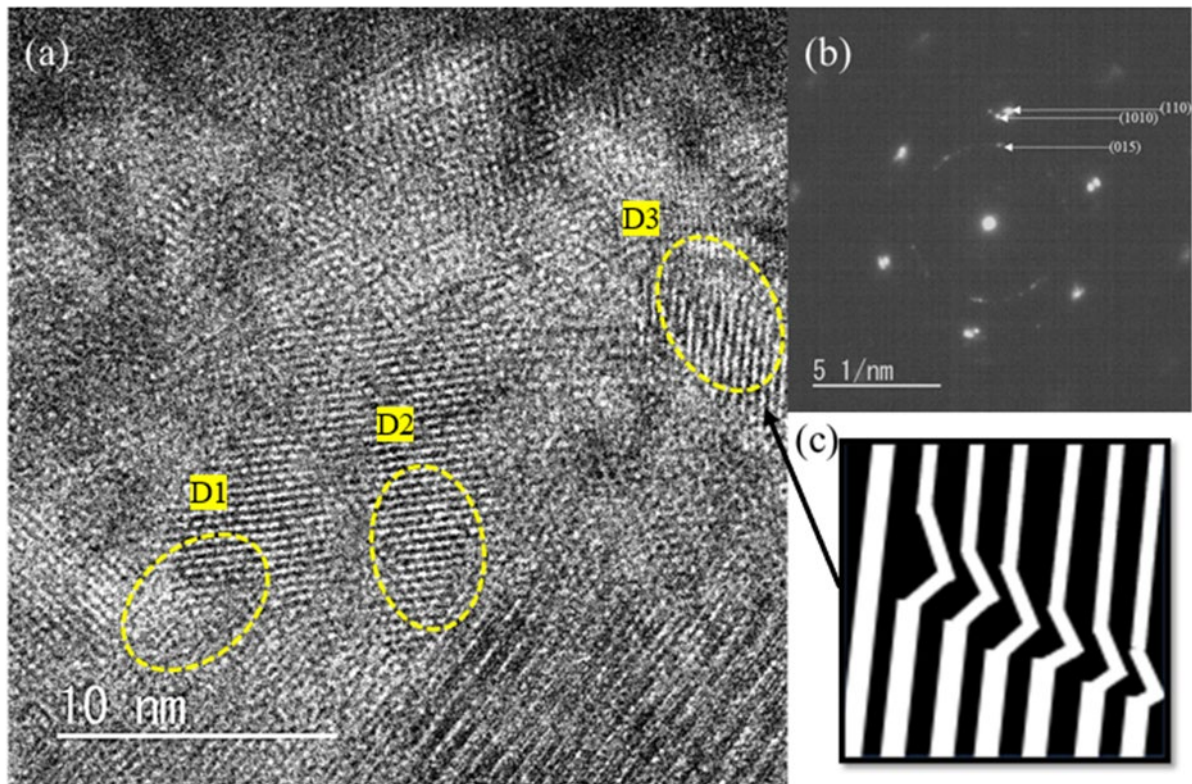


Fig. 6. (a) TEM image of 3wt% Graphene/ Bi_2Te_3 (b) SAED Pattern (c) Illustrated defects based on the TEM image

The defects formation in the synthesized nanocomposite films plays a crucial role in modifying the thermal properties of the material by influencing the phonon scattering, and thus affects the sample's thermal conductivity. The identified stacking faults induced phonon scattering within interfaces, leading to a reduction in lattice thermal conductivity [35-36]. The quantized lattice vibrations responsible for heat transfer are scattered with these stacking faults, disrupting their coherent propagation and reducing their ability to transport heat effectively. The formation of a lot of grain boundaries due to smaller grain size of the Graphene/ Bi_2Te_3 nanocomposite films increased the density of interfaces in the material, which enhances phonon scattering [37]. The increased density of grain boundaries provides additional scattering sites for phonons, impeding their coherent propagation and reducing the thermal conductivity of the material [37]. As the grain size decreases, the density of grain boundaries increases, leading to enhanced phonon scattering and reduced thermal conductivity [36]. The combination of stacking faults and grain boundary scattering can have a synergistic effect on phonon scattering in Graphene/ Bi_2Te_3 nanocomposites. Report indicate that the observed giant reduction in thermal conductivity in Bi_2Te_3 nanostructures is due to the multi-scale phonon scattering caused by a combination of stacking faults, lattice dislocations, and grain boundary scattering [35]. The coexistence of hierarchical defect structures and dislocations in nanostructured Bi_2Te_3 TE systems contributes to the multi-scale phonon scattering, resulting in a significant reduction in thermal conductivity [35].

4. Conclusions

This article presents the synthesis process of a new electrodeposited Graphene/ Bi_2Te_3 nanocomposite film. To date, the use of graphene nanomaterials as the nano inclusion in Bi_2Te_3 matrix has not been fully investigated in film condition especially the one that is synthesized with

electrodeposition process. The nanocomposite films were synthesized using a potentiostatically pulsed electrochemical deposition by varying the graphene concentration in the electrolytes and the synthesized films of up to 3 wt.% of graphene nanoparticles were produced. It was found that as higher graphene nanoparticles deposited in the nanocomposite film, the grain size became smaller and the nanostructure experienced significant defects. The average grain size of the Graphene/Bi₂Te₃ TE films decreased nearly 40% as compared to the pristine Bi₂Te₃ film. The grain size reduction and the defects existence may benefit on the overall TE performance (ZT) through the electron and phonon scattering. Stacking faults and grain boundaries significantly affect phonon scattering in Graphene/Bi₂Te₃ nanocomposites, leading to a reduction in lattice thermal conductivity. The presence of stacking faults introduces additional scattering centers, while the increased density of grain boundaries provides more scattering sites for phonons. These defects play a crucial role in modifying the thermal properties of the material and can be utilized to optimize the TE performance of Bi₂Te₃ nanocomposites, which will be experimentally confirmed by future work.

Acknowledgement

Authors are grateful to Universiti Teknikal Malaysia Melaka for the financial support through PJP/2020/FKP/PP/S01757. Part of this work was performed in the Shibaura Institute of Technology.

References

- [1] Zhu, Sijing, Zheng Fan, Baoquan Feng, Runze Shi, Zexin Jiang, Ying Peng, Jie Gao, Lei Miao, and Kunihito Koumoto. "Review on wearable thermoelectric generators: from devices to applications." *Energies* 15, no. 9 (2022): 3375.
- [2] Bisht, Neha, Priyesh More, Pawan Kumar Khanna, Reza Abolhassani, Yogendra Kumar Mishra, and Morten Madsen. "Progress of hybrid nanocomposite materials for thermoelectric applications." *Materials Advances* 2, no. 6 (2021): 1927-1956. <https://doi.org/10.1039/D0MA01030H>
- [3] Liu, Bin, Jizhu Hu, Jun Zhou, and Ronggui Yang. "Thermoelectric transport in nanocomposites." *Materials* 10, no. 4 (2017): 418. <https://doi.org/10.3390/ma10040418>
- [4] Kul'bachinskii, V. A. "Nanostructuring and creation of nanocomposites as a promising way to increase thermoelectric efficiency." *Nanotechnologies in Russia* 14 (2019): 334-345. <https://doi.org/10.1134/S1995078019040098>
- [5] Tang, Xinfeng, Ziwei Li, Wei Liu, Qingjie Zhang, and Ctirad Uher. "A comprehensive review on Bi₂Te₃-based thin films: thermoelectrics and beyond." *Interdisciplinary Materials* 1, no. 1 (2022): 88-115. <https://doi.org/10.1002/idm2.12009>
- [6] Chiba, Tomoyuki, Hayato Yabuki, and Masayuki Takashiri. "High thermoelectric performance of flexible nanocomposite films based on Bi₂Te₃ nanoplates and carbon nanotubes selected using ultracentrifugation." *Scientific Reports* 13, no. 1 (2023): 3010. <https://doi.org/10.1038/s41598-023-30175-0>
- [7] Samat, Khairul Fadzli, Nguyen Huu Trung, and Takahito Ono. "Enhancement in thermoelectric performance of electrochemically deposited platinum-bismuth telluride nanocomposite." *Electrochimica Acta* 312 (2019): 62-71. <https://doi.org/10.1016/j.electacta.2019.04.139>
- [8] Li, Peigen, Jigui Shi, Xuelian Wu, Junqin Li, Lipeng Hu, Fusheng Liu, Yu Li, Weiqin Ao, and Chaohua Zhang. "Interfacial engineering of solution-processed Bi₂Te₃-based thermoelectric nanocomposites via graphene addition and liquid-phase-sintering process." *Chemical Engineering Journal* 440 (2022): 135882. <https://doi.org/10.1016/j.cej.2022.135882>
- [9] Ahmad, Kaleem, C. Wan, M. A. Al-Eshaikh, and A. N. Kadachi. "Enhanced thermoelectric performance of Bi₂Te₃ based graphene nanocomposites." *Applied Surface Science* 474 (2019): 2-8. <https://doi.org/10.1016/j.apsusc.2018.10.163>
- [10] Du, Yong, Jia Li, Jiayue Xu, and Per Eklund. "Thermoelectric properties of reduced graphene oxide/Bi₂Te₃ nanocomposites." *Energies* 12, no. 12 (2019): 2430. <https://doi.org/10.3390/en12122430>
- [11] Ahmad, Kaleem, C. Wan, M. A. Al-Eshaikh, and A. N. Kadachi. "Enhanced thermoelectric performance of Bi₂Te₃ based graphene nanocomposites." *Applied Surface Science* 474 (2019): 2-8. <https://doi.org/10.1016/j.apsusc.2018.10.163>
- [12] Li, Shuankui, Tianju Fan, Xuerui Liu, Fusheng Liu, Hong Meng, Yidong Liu, and Feng Pan. "Graphene quantum dots embedded in Bi₂Te₃ nanosheets to enhance thermoelectric performance." *ACS applied materials & interfaces* 9, no. 4 (2017): 3677-3685. <https://doi.org/10.1021/acsami.6b14274>

- [13] Kumar, Sunil, Simrjit Singh, Punit Kumar Dhawan, R. R. Yadav, and Neeraj Khare. "Effect of graphene nanofillers on the enhanced thermoelectric properties of Bi₂Te₃ nanosheets: elucidating the role of interface in de-coupling the electrical and thermal characteristics." *Nanotechnology* 29, no. 13 (2018): 135703. <https://doi.org/10.1088/1361-6528/aaa99e>
- [14] Perumal, Suguna, Raji Atchudan, and In Woo Cheong. "Recent studies on dispersion of graphene-polymer composites." *Polymers* 13, no. 14 (2021): 2375. <https://doi.org/10.3390/polym13142375>
- [15] Zhao, Wei, Abhilash Sugunan, Thomas Gillgren, Johan A. Larsson, Zhi-Bin Zhang, Shi-Li Zhang, Niklas Nordgren, Jens Sommertune, and Anwar Ahniyaz. "Surfactant-free stabilization of aqueous graphene dispersions using starch as a dispersing agent." *ACS omega* 6, no. 18 (2021): 12050-12062. <https://doi.org/10.1021/acsomega.1c00699>
- [16] Ma, Yifei, Jiemin Han, Mei Wang, Xuyuan Chen, and Suotang Jia. "Electrophoretic deposition of graphene-based materials: A review of materials and their applications." *Journal of Materiomics* 4, no. 2 (2018): 108-120. <https://doi.org/10.1016/j.jmat.2018.02.004>
- [17] Orrill, Michael, Dustin Abele, Michael J. Wagner, and Saniya LeBlanc. "Sterically Stabilized Multilayer Graphene Nanoshells for Inkjet Printed Resistors." *Electronic Materials* 2, no. 3 (2021): 394-412. <https://doi.org/10.3390/electronicmat2030027>
- [18] Texter, John. "Graphene dispersions." *Current Opinion in Colloid & Interface Science* 19, no. 2 (2014): 163-174. <https://doi.org/10.1016/j.cocis.2014.04.004>
- [19] Eichhorn, Stephen J., Libo Deng, Robert J. Young, and Ian A. Kinloch. "Electrospun cellulose fibres for carbon fibre precursors." In *ABSTRACTS OF PAPERS OF THE AMERICAN CHEMICAL SOCIETY*, vol. 247. American Chemical Society, 2014. <https://doi.org/10.1021/acs.langmuir.5b04219>
- [20] Johnson, David W., Ben P. Dobson, and Karl S. Coleman. "A manufacturing perspective on graphene dispersions." *Current Opinion in Colloid & Interface Science* 20, no. 5-6 (2015): 367-382. <https://doi.org/10.1016/j.cocis.2015.11.004>
- [21] Chen, Yue-Xing, Jun-Ze Zhang, Mohammad Nisar, Adeel Abbas, Fu Li, Guang-Xing Liang, Ping Fan, and Zhuang-Hao Zheng. "Realizing high thermoelectric performance in n-type Bi₂Te₃ based thin films via post-selenization diffusion." *Journal of Materiomics* (2023). <https://doi.org/10.1016/j.jmat.2023.01.003>
- [22] Recatala-Gomez, Jose, Pawan Kumar, Ady Suwardi, Anas Abutaha, Iris Nandhakumar, and Kedar Hippalgaonkar. "Direct measurement of the thermoelectric properties of electrochemically deposited Bi₂Te₃ thin films." *Scientific Reports* 10, no. 1 (2020): 17922. <https://doi.org/10.1038/s41598-020-74887-z>
- [23] Lin, Chin-Wei, Kuang-Lu Huang, Kai-Wei Chang, Jan-Han Chen, Kuen-Lin Chen, and Chiu-Hsien Wu. "Ultraviolet photodetector and gas sensor based on amorphous In-Ga-Zn-O film." *Thin Solid Films* 618 (2016): 73-76. <https://doi.org/10.1016/j.tsf.2016.12.047>
- [24] Ashfaq, Arslan, Michael M. Sabugaa, Mongi Ben Moussa, N. Almousa, Elsammani Ali Shokralla, Rey Y. Capangpangan, Arnold C. Alguno, Md Amzad Hossain, Abdulaziz M. Alanazi, and Mohamed Abboud. "High thermoelectric power factor of Sr doped Bi₂Te₃ thin film through energy filtering effect." *International Communications in Heat and Mass Transfer* 143 (2023): 106719. <https://doi.org/10.1016/j.icheatmasstransfer.2023.106719>
- [25] Hosokawa, Yuichi, Koji Tomita, and Masayuki Takashiri. "Growth of single-crystalline Bi₂Te₃ hexagonal nanoplates with and without single nanopores during temperature-controlled solvothermal synthesis." *Scientific Reports* 9, no. 1 (2019): 10790. <https://doi.org/10.1038/s41598-019-47356-5>
- [26] Li, Shanghua, Shuo Zhang, Zeming He, Muhammet Toprak, Christian Stiewe, Mamoun Muhammed, and Eckhard Müller. "Novel solution route synthesis of low thermal conductivity nanocrystalline bismuth telluride." *Journal of Nanoscience and Nanotechnology* 10, no. 11 (2010): 7658-7662. <https://doi.org/10.1166/jnn.2010.2775>
- [27] Suh, Hoyoung, Jinseong Noh, Ji-Hyun Lee, Seok-Hoon Lee, Nosang V. Myung, Kimin Hong, and Jin-Gyu Kim. "Morphological Evolution of Te and Bi₂Te₃ Microstructures during Galvanic Displacement of Electrodeposited Co Thin Films." *Electrochimica Acta* 255 (2017): 1-8. <https://doi.org/10.1016/j.electacta.2017.09.049>
- [28] Humphry-Baker, Samuel A., and Christopher A. Schuh. "Grain growth and structural relaxation of nanocrystalline Bi₂Te₃." *Journal of Applied Physics* 116, no. 15 (2014). <https://doi.org/10.1063/1.4898320>
- [29] Ivanov, Oleg, Oxana Maradudina, and Roman Lyubushkin. "Grain size effect on electrical resistivity of bulk nanograined Bi₂Te₃ material." *Materials Characterization* 99 (2015): 175-179. <https://doi.org/10.1016/j.matchar.2014.12.001>
- [30] Battogtokh, Jugdersuren, Brian T. Kearney, James C. Culbertson, Christopher N. Chervin, Michael B. Katz, Rhonda M. Stroud, and Xiao Liu. "The effect of ultrasmall grain sizes on the thermal conductivity of nanocrystalline silicon thin films." *Communications Physics* 4, no. 1 (2021). <https://doi.org/10.1038/s42005-021-00662-9>
- [31] Takashiri, M., K. Miyazaki, S. Tanaka, J. Kurosaki, D. Nagai, and H. Tsukamoto. "Effect of grain size on thermoelectric properties of n-type nanocrystalline bismuth-telluride based thin films." *Journal of Applied*

- Physics 104, no. 8 (2008). <https://doi.org/10.1063/1.2990774>
- [32] Walck, Scott D. "Recipes for Consistent Selected Area Electron Diffraction Results: Part 2: Recording the SAED Pattern." *Microscopy Today* 28, no. 3 (2020): 54-59. <https://doi.org/10.1017/S1551929520000887>
- [33] Li, X. Z. "JECPCSAED, a Computer Program for Quantification of SAED Patterns." *Microscopy and Microanalysis* 20, no. S3 (2014): 1486-1487. <https://doi.org/10.1017/S1431927614009167>
- [34] Sun, Cheng, Erich Müller, Matthias Meffert, and Dagmar Gerthsen. "Analysis of crystal defects by scanning transmission electron microscopy (STEM) in a modern scanning electron microscope." *Advanced Structural and Chemical Imaging* 5 (2019): 1-9. <https://doi.org/10.1186/s40679-019-0065-1>
- [35] Vijay, V., S. Harish, J. Archana, and M. Navaneethan. "Synergistic effect of grain boundaries and phonon engineering in Sb substituted Bi₂Se₃ nanostructures for thermoelectric applications." *Journal of Colloid and Interface Science* 612 (2022): 97-110. <https://doi.org/10.1016/j.jcis.2021.12.027>
- [36] Singh, B. K., and L. K. Sharma. "Scattering of phonon by stacking faults and dislocation cores in plastically deformed LiF crystal: An analysis." *International Journal of Modern Physics B* 33, no. 23 (2019): 1950259. <https://doi.org/10.1142/S021797921950259X>
- [37] Morimoto, Masayuki, Shoya Kawano, Koji Miyazaki, and Satoshi Iikubo. "Structural stability and electronic property evaluations for different Bi₂Te₃ (0 0 1) termination surfaces." *Applied Surface Science* 525 (2020): 146454. <https://doi.org/10.1016/j.apsusc.2020.146454>